IEEE Photonics Journal
An IEEE Photonics Society Publication

Open Access

Intensity and Wavelength-Division Multiplexing Fiber Sensor Interrogation Using a Combination of Autoencoder Pre-Trained Convolution Neural Network and Differential Evolution Algorithm

Volume 13, Number 1, February 2021

Po-Han Chiu
Yu-Shen Lin
Yibeltal Chanie Manie
Jyun-Wei Li
Ja-Hon Lin
Peng-Chun Peng

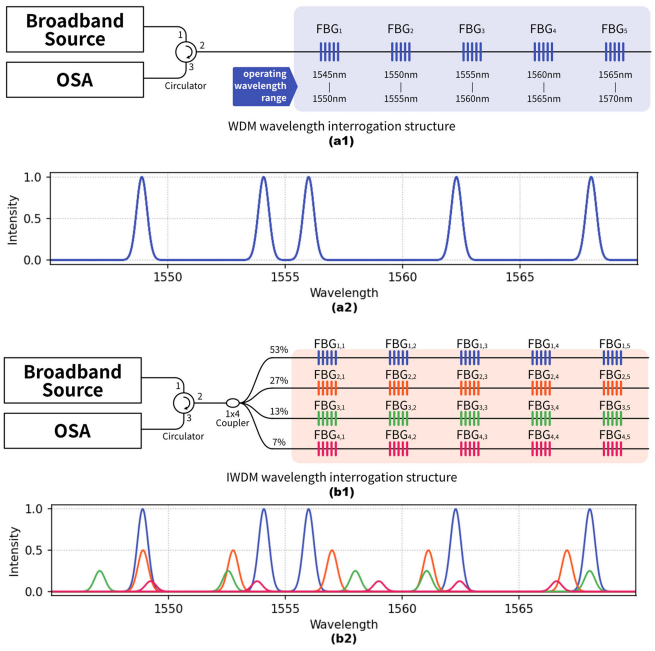

DOI: 10.1109/JPHOT.2021.3050298

Intensity and Wavelength-Division Multiplexing Fiber Sensor Interrogation Using a Combination of Autoencoder Pre-Trained Convolution Neural Network and Differential Evolution Algorithm

Po-Han Chiu, Yu-Shen Lin, Yibeltal Chanie Manie, Jyun-Wei Li, Ja-Hon Lin, and Peng-Chun Peng

Department of Electro-Optical Engineering, National Taipei University of Technology, Taipei 10608, Taiwan

DOI:10.1109/JPHOT.2021.3050298

Manuscript received December 25, 2020; accepted January 5, 2021. Date of publication January 11, 2021; date of current version January 21, 2021. This work was supported by the Ministry of Science and Technology, Taiwan, under Grants MOST 108-2221-E-027 -040 -MY2 and MOST 109-2813-C-027-017-E. Corresponding author: Peng-Chun Peng (e-mail: pcpeng@ntut.edu.tw).

Abstract: This paper proposes a new fiber Bragg grating central wavelength interrogation system by combining evolutionary algorithm and machine learning techniques integrated with an unsupervised autoencoder (AE) pre-training strategy. The proposed unsupervised AE pre-training convolution neural network (CNN) allows training of the convolutional layers independently from a regression task in order to learn a new data representation and give better generalization. It is also used to improve the system accuracy by four times without extra-labeled data. Moreover, AE is combined with a differential evolutionary (DE) algorithm to automate the human labeling task. The proposed autoencoder pre-training convolution neural network and differential evolutionary (AECNNDE) interrogation system achieve good accuracy and can speed-up the computational time by a maximum of 30 times than DE algorithm.

Index Terms: Intensity and wavelength division multiplexing (IWDM), Fiber Bragg gratings (FBG), Machine learning.

1. Introduction

The fiber sensor has advantages in multiple measurement fields to measure different parameters [1]–[6]. Fiber Bragg grating (FBG) sensor is a type of fiber sensor that commonly used to measure temperature, strain, vibration, pressure, and several other physical quantities [7]–[10]. The strain-sensing concept of FBG sensor can be determined by the shift of the peak wavelength of FBG due to the variation of physical parameters [11], [12]. In FBG sensor system, a self-healing structure is a good solution to increase the reliability and survivability issue of the sensor network [13]. Furthermore, one of the most important benefits of FBG sensors is their multiplexing and wavelength encoding capability [14], [15]. In a quasi-distributed sensor system, several FBG sensors can be multiplexed in a single cable using different multiplexing techniques. Multiplexing of FBG sensor is used to reduce the operation and installation costs of quasi-distributive strain measurements. Thus, FBG integrated with wavelength division multiplexing (WDM) technique is

one of the most important technique that hugely increases the number of sensors and monitor different parameters simultaneously. However, the reflection spectra of cascading FBG sensors cannot overlap in the WDM system, which limits the number of sensors multiplexed in the sensor system.

Recently, to overcome this problem and to further increasing the number of sensors in the system, the intensity and wavelength division multiplexing (IWDM) method was proposed [16]–[19]. In the IWDM system, multiple WDM systems are multiplexed together with different reflection intensity. Thus, IWDM can improve the multiplexing capacity of the FBG sensor system and increasing the number of FBG sensors by more than twice as traditional WDM techniques [18], [19]. Nevertheless, in IWDM, overlapping of cascading FBGs causes crosstalk that is challenging to distinguish the central wavelength of each sensor. Most recently, different algorithms, such as evolution-based algorithms can be applied to analyze the spectrum and measure the central wavelength from the overlap spectra [20]. However, in evolutionary algorithms, the computational cost increases exponentially when the number of FBGs in the sensor system increase. To solve this issue, machine learning-based central wavelength interrogation algorithms are proposed to provide high-speed inferences and parallel computing.

Moreover, while machine learning drastically improving the performance of the system, a tremendous amount of data is required for training the network. In addition, traditional machine learning algorithms has less learning capacity and less flexibility, require long computational time and the accuracy was not promising, which is not ideal for real-time parameters monitoring. In the previously proposed convolutional neural network (CNN) based machine learning interrogation system [21], 24000 samples are used to train the model. This kind of training data is often hard to prepare for a real sensing scenario and only fits into one case. Therefore, in this paper, we introduce an unsupervised autoencoder (AE) pre-training strategy to improve the system accuracy by four times without extra labeled data. This allows training of the convolutional layers independently from a regression task in order to learn a new data representation and give better generalization. Thus, our proposed model consists of multiple layers that have excellent capabilities to deal with complex and nonlinear data. Moreover, AE is combining with an evolutionary algorithm to automate the human labeling task and automatically extract features of the long sequence spectra data. The experimental result proves that the proposed autoencoder-convolutional neural network and differential evolution (AECNNDE) interrogation system achieving good accuracy and speed-up the computational time in a maximum of 30 times while reducing the difficulty of setting up the sensing system. Furthermore, our proposed structure can increase the reliability of large-scale FBG sensor system.

The rest part of this paper is organized as follows: the operational principle and experimental setup is described in Section 2. In Section 3, the experimental results is presented. Finally, in Section 4 the conclusion part is presented.

2. Operation Principle and Experiment Setup

2.1 Fiber Bragg Grating(FBG) and IWDM Principles

As illustrated in Fig. 1, in an ideal IWDM system, a broadband light source feds into a circulator and then split into *N* rows using couplers. Each row has a different intensity ratio and consisting of *m* number of FBG sensors labeled with $\text{FBG}_{N,m}$. When the light goes through each FBG, a reflection spectrum is generated from each FBG depends on the strain we applied. A different uniform strain is applied in FBG using a micro translation stage and the reflection spectra of FBGs at each strain value is captured and recorded using an optical spectrum analyzer (OSA). Then, the recorded reflection signal of FBGs sends to the computer for further data processing. Suppose the reflection spectra from a single $\text{FBG}_{N,m}$ having a Gaussian shape, the reflection spectrum can be formulated

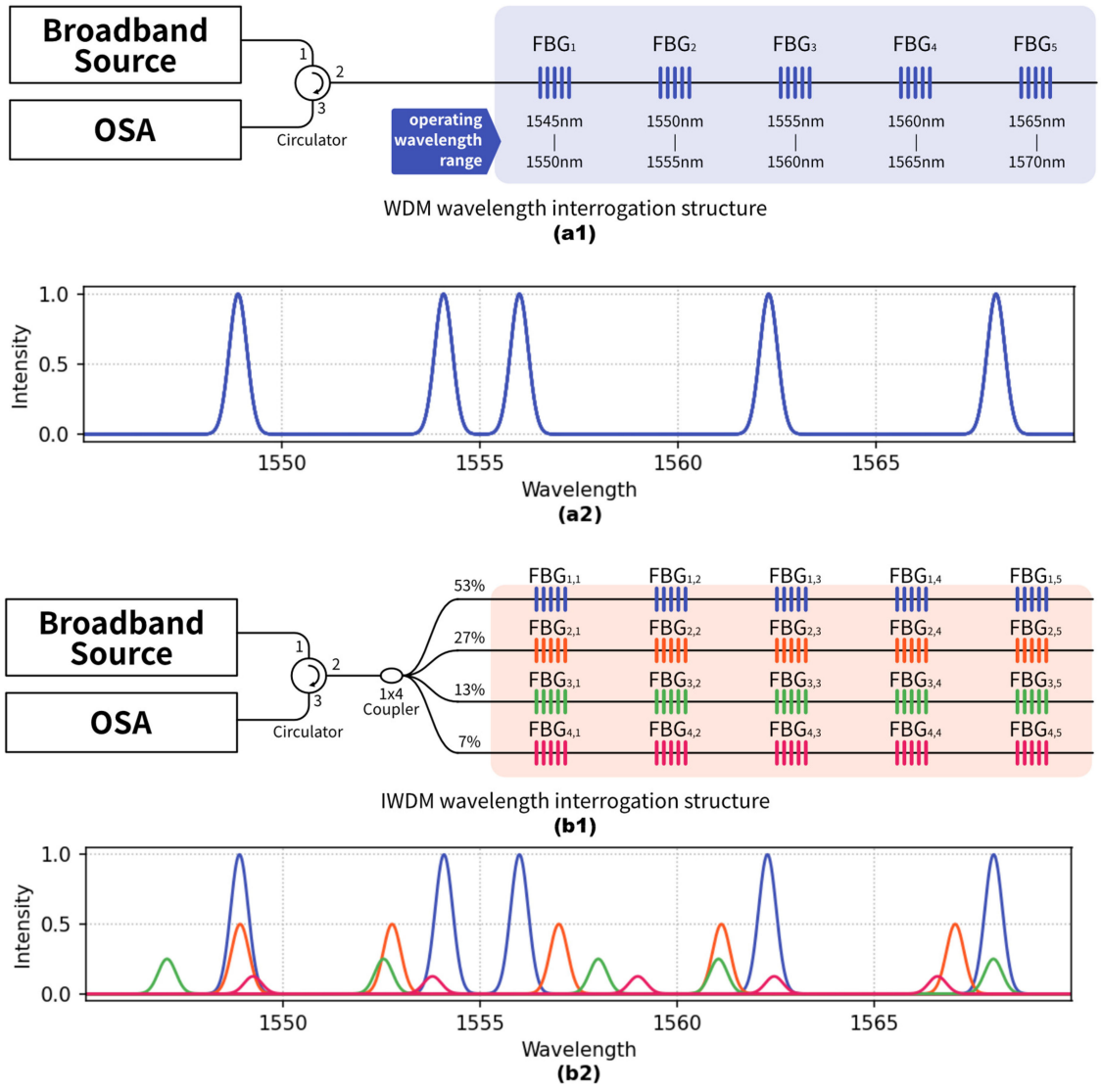

Fig. 1. Schematic diagram of FBG sensor system (a1) using WDM wavelength interrogation structure (a2) Spectrum of WDM (b1) using IWDM wavelength interrogation structure (b2) Spectrum of IWDM.

by the formula (1):

$$R\ (\lambda, \lambda_{N,m}) = I_p\ \exp\left[-4ln2\ \times\ \left(\frac{\lambda - \lambda_{N,m}}{\Delta\lambda_B}\right)^2\right] \tag{1}$$

Where $\lambda_{N,\mathrm{m}}$ is the central wavelength that depends on the measurands, I_p is the reflected peak intensity, $\Delta\lambda_{\mathrm{B}}$ represents the full width at half maximum (FWHM) of the FBG. I_p and $\Delta\lambda_{\mathrm{B}}$ are the two important parameters to configure the IWDM system, $\lambda_{N,\mathrm{m}}$ is the value which we need to solve by our system.

2.2 Interrogation System

Though the IWDM method is useful in sensing systems, any damage or link failure into the complex coupler setup might influence the coupling ratio and the system no longer works. Fig. 2(a) shows

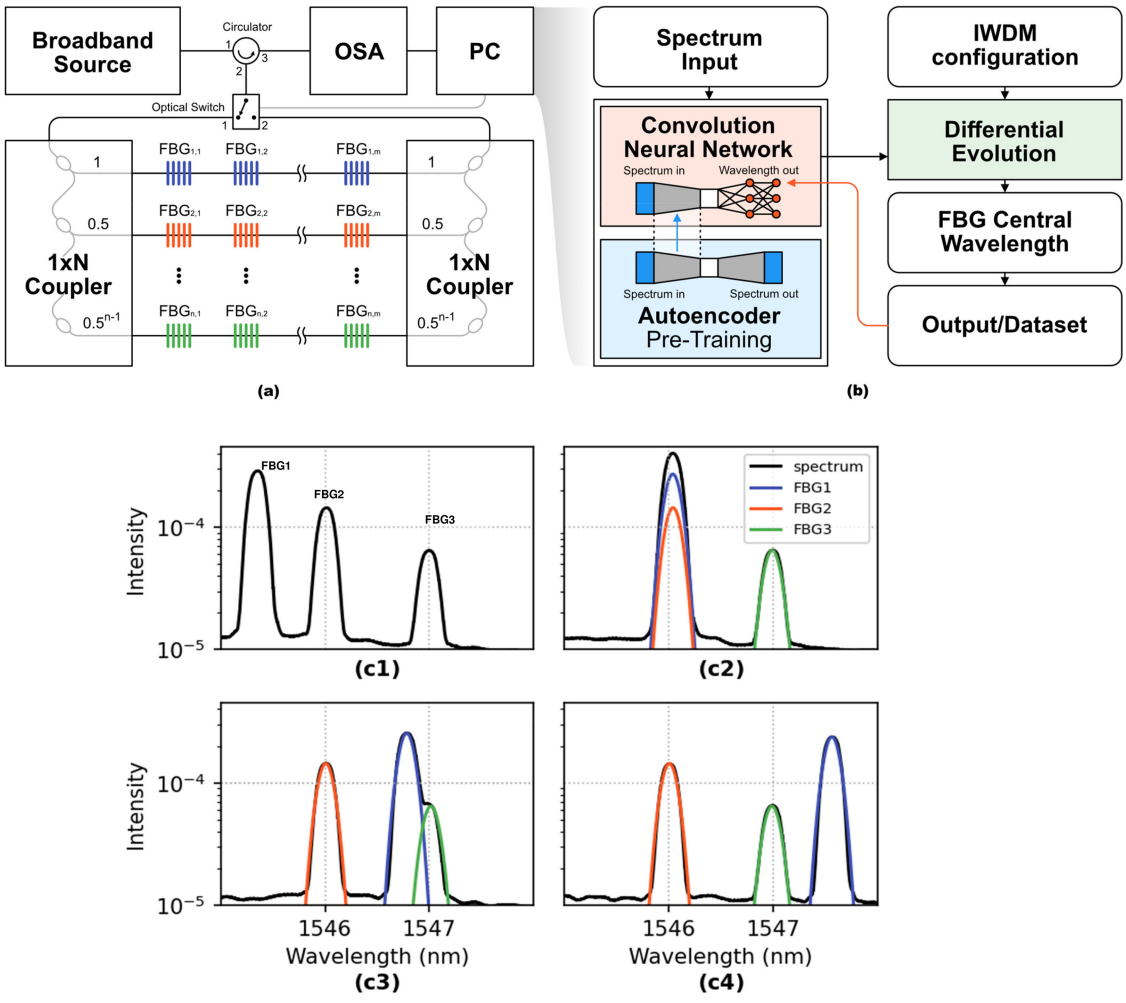

Fig. 2. (a) Experiment setup. (b) Proposed wavelengths interrogation system (c1) The reflection spectrum of three FBG (c2) Reflection spectrum reconstructed when FBG1 and FBG2 is completely overlapped (c3) Reflection spectrum reconstructed when FBG1 and FBG3 is partially overlapped (c4) Three FBGs' central wavelengths are separated from each other.

our experimental setup of the proposed IWDM FBG sensor system. As shown in the figure, by adding an identical coupler setup to each side of the IWDM system, the risks of FBG sensor system failures are reduced. Thus, when a link failure occurs, a computer-controlled optical switch can provide self-healing ability by dynamically reconfiguring and rerouting the signal into another transmission path [22]–[24].

In this work, we demonstrate a novel interrogation technique to detect the central wavelengths from the overlapping spectra using a promising deep learning technique, AECNNDE. The wavelength demodulation of FBG network is regarded as a nonlinear regression problem and the proposed AECNNDE model is a sequence model that can deal with nonlinear regression problems. The proposed wavelength interrogation system is depicted in Fig. 2(b).

As shown in the figure, the input spectrum that is the reflection spectra of FBGs is obtained from OSA and pre-processed using personal computer (PC). Thus, the input spectrum (long sequence spectra) is used as training data. The training data is automatically labeled by DE and used to pre-train the CNN model. In the proposed model, feature extraction of the long sequence spectra

data input would be done by 1D convolutional layers. 1D convolutional layer creates a convolution kernel that is convolved with the layer input over a single spatial (or temporal) dimension to produce a tensor of outputs. Thus, we provide an input_shape argument (tuple of integers (1, 1000)) for sequences of N number of length sequence of 1000-dimensional vectors. Then, after training the AE pre-trained CNN system by adjusting different parameters like epoch number, batch size and other parameters; the AE pre-trained CNN will evaluate the spectrum and obtain the central wavelengths of each FBGs. Then, the generated wavelength values from CNN serve as the initial input of the DE algorithm. As a result, a DE algorithm with a given IWDM configuration including I_p and $\Delta\lambda_B$ will reconstruct the spectrum by formula (1) to find $\lambda_{N,m}$. Then, the reconstructed spectrum is comparing with the actual (measured) spectrum in order to check the difference, and further improve the accuracy after multiple evolution iterations. Finally, we get the accurate central wavelengths of the FBGs $\lambda_{N,m}$, and fed back to our CNN network for continuous training of the CNN network. Fig. 2(c1) shows the original spectrum of three FBGs. When strain is applied to FBG1, there are three circumstances of spectra such as the reflection spectrum being completely overlapped, partially overlapped, or completely separated, as shown in Fig. 2(c2-c4). Hence, when the spectra of FBGs are completely overlapped, the conventional peak detection method is very challenging to identify with the crosstalk of spectra and cannot accurately identify the Bragg wavelength of each FBG. As shown in Fig. 2(c2-c4), our proposed model overcomes the crosstalk difficulties and can accurately measure the Bragg wavelength of each FBG.

3. Experiment Result

The performance of the proposed system is verified using two scenarios. The first scenario is using three FBG sensors, and the second scenario is using seven FBG sensors. In the first scenario, the central wavelengths of FBG1, FBG2, and FBG3 sensors are 1545.35 nm, 1546 nm, 1547 nm, respectively. The FWHM of three FBGs is 0.1975 nm. The reflection spectrum measured by OSA has a sampling resolution of 2.5 pm. During the experiment, when applying a distinct strain to FBG1, the central wavelength of FBG1 is shifted from 1545.35 nm to 1547.56 nm with 13 strain steps. The reflection spectrum of three FBGs at different strain steps is shown in Fig. 3(a).

As shown in the Fig. 3, the overlapping spectra of FBGs introduces crosstalk, which reduces the overall sensor network performance significantly. Thus, to solve this overlap problem, the combined long sequence spectrum is fed to the model as input, and the Bragg wavelengths of each FBG are extracted from the overlapped FBG spectra. In the proposed model, we employed 1D spectra data, where the wavelengths range are mapped to indices of the array. The model was trained using 1000 samples that are calculated using (1). To train the model, the batch size and learning rate used were 1000 and 0.001 respectively. Moreover, The Adam optimization algorithm was used to reduce the loss between the actual central wavelength of each FBG and the outputs of the proposed model. The proposed CNN network has 4 layers of encoders and decoders. Encoders have 4 groups of Conv1D and max-pooling, while Decoder has 4 groups of Conv1D and Upsampling. A Conv1D is very effective for deriving features from the overall time series of the sensor dataset. After each convolution layer (4 layer), the max-pooling layer will downsample the input or reduce the length of the data by two for the first three layer and reduce by five for the last layer, while the upsampling layer will upsample the input by five for the first layer and reduce by two for the last three layer. The activation function of exponential Linear Unit (ELU) is added between each layer to reduce vanishing gradient and exploding gradients problem in models with a large number of layers. Using ELU leads to lower training times and higher accuracies in Neural Networks (NN) as compared to Rectified Linear Unit (ReLU) and its variants. After all convolution and max pooling is process completed, the dense connected layer of three layer with a dense unit of 50, 25, 5, respectively is executed. The activation function of the dense layer is also ELU. The proposed methods output result, which is the detected Bragg wavelength of each FBGs at different strain steps, is shown in Fig. 3(b). For measuring the Bragg wavelength detection performance of the proposed approach,

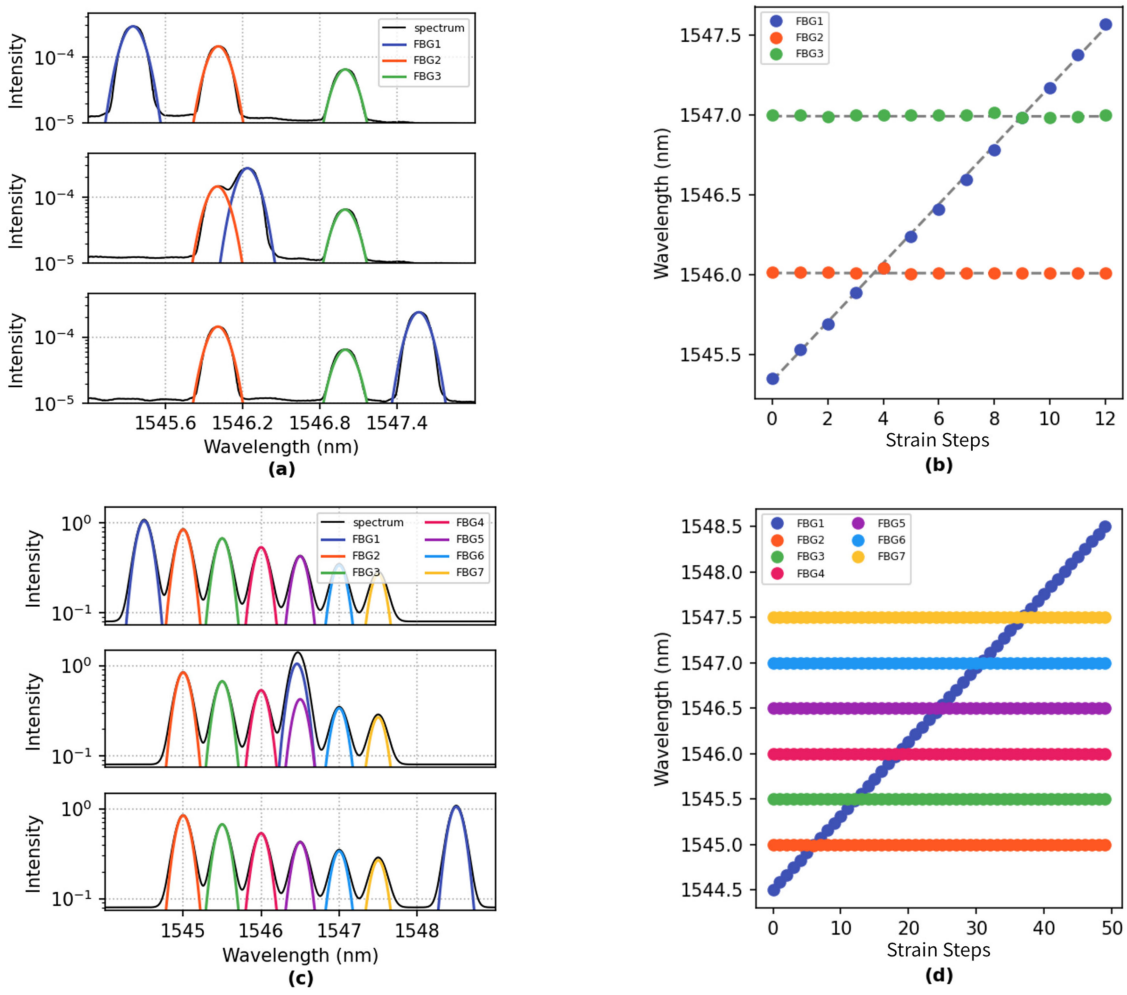

Fig. 3. (a) detected spectra of three FBGs using the proposed model (b) The detected Bragg wavelengths of three FBGs, when different strain was applied to FBG1 (c) Simulation spectra of seven FBGs using the proposed model (d) Simulation Bragg wavelengths of seven FBGs, when different strain was applied to FBG1.

we use RMSE evaluation methods, defined as follows:

$$RMSE = \sqrt{\frac{\sum_{i=1}^{n} (y_i - y)^2}{n}} \tag{2}$$

Where n, y_i , and y are the number of predicted values, the actual value, and the predicted value, respectively. Thus, the average root-mean-square error (RMSE) performance of the proposed model is 13.97 pm.

In the second scenario, we try to approve the capability of the proposed system when the sensors number increases. As shown in Fig. 3(c), the computer-simulated spectrum data of seven FBGs. The central wavelengths of FBGs are uniformly distributed from 1544 nm to 1548 nm. When strain is applied to FBG1, the central wavelength of FBG1 moves from 1544.5 nm to 1548.5 nm with 50 strain steps. Moreover, the intensity of FBG1 is set to be 1 and the intensity of n^{th} FBG is 0.83 times lower from the previous FBG. The detected central wavelength output result of the proposed system is shown in Fig. 3(d). As shown in the figure, the system has a reliable accuracy in the measurement of each FBG's central wavelength even when the sensor number increase or in a

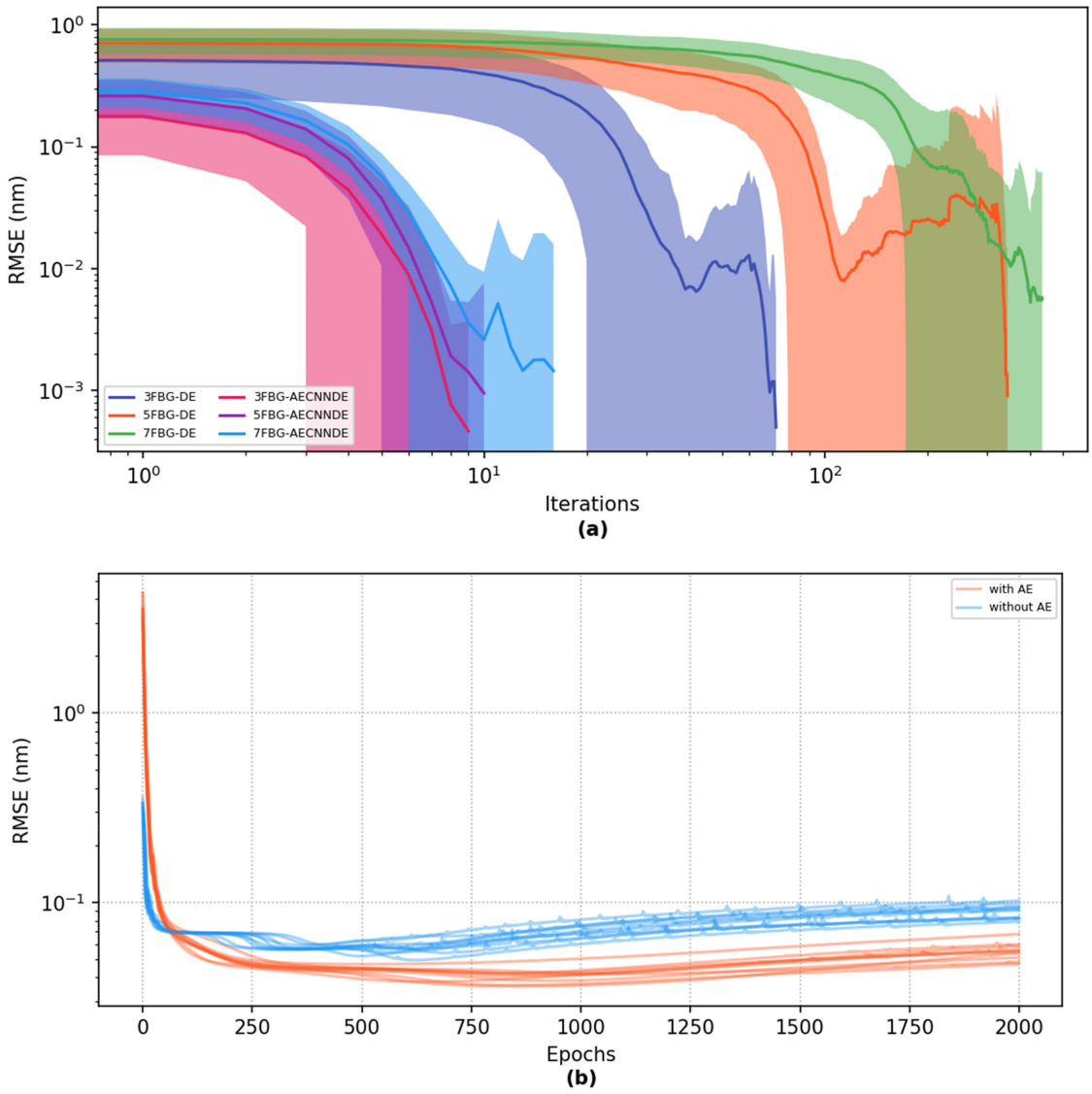

Fig. 4. (a) Iteration times comparison of DE algorithm and our system (b) Training epochs on our system and original CNN with its RMSE.

complex FBG sensor system. The root-mean-square error (RMSE) performance of the proposed system in the second scenario is 1.003 pm. Furthermore, if our proposed system can solve the overlap of $\lambda 1$, $\lambda 2$, $\lambda 3$ and other sensors when strain is applied to $\lambda 1$ sensor, it is practically know that it can also solve the overlap of $\lambda 1$, $\lambda 2$, $\lambda 3$ and other sensors even when strain is applied to $\lambda 2$ or $\lambda 3$ or other sensors. Because when strain is applied to $\lambda 1$ and overlap is occurred between the spectra of λ 1, λ 2, λ 3 and other sensors, the overlap spectra of two or more sensors is the sum of each FBG sensors output intensity, which is the same as when strain is applied to $\lambda 2$ or $\lambda 3$ sensors. So, in this paper, to prove our proposed system performance, we just show the case when strain is applied to $\lambda 1$ and measure the Bragg wavelength of each FBGs. As discussed above when strain is applied to $\lambda 1$ sensor, our proposed system can measure the Bragg wavelength of each FBGs even when the spectra of two or three FBGs are overlapped. Thus, it is sure that it also work when strain is applied to either $\lambda 2$ or $\lambda 3$ or $\lambda 4$ or other sensors.

Moreover, to test and compare the efficiency improvement of our proposed system and pure DE algorithm, we collect 3FBG, 5FBG, and 7FBG simulated spectrum data having the same FWHM but different intensity ratios. As shown in Fig. 4(a), our proposed system requires fewer iterations than pure DE to get the same RMSE. Especially, when the FBG number increases and spectrum overlap occurs, pure DE would take more iterations while our proposed method takes a few iterations in the case of 3FBG, 5FBG, and 7FBG sensors. In our proposed AECNNDE model, the average iteration time of 3FBG, 5FBG, and 7FBG sensors are reduced by 7, 30, and 27 times, respectively. Therefore, since the time cost of DE is the most concerned issue, instead of random initializing the DE algorithm, using a CNN network can give a better measurement performance and the iterations times are decreased.

Furthermore, in a real sensing system, the real training data for real measurements is far less than the data requiring for training a model and more difficult to get the labeled data. When the number of labeled data is small, the generalization performance of the model becomes poor. To improve the generalization performance of the proposed model even though less training data is given, AE is added to pre-train the proposed model. In this paper, we use 1000 training data, 9000 testing data to test our pre-trained CNN and original CNN model. The reason for using less training data is to see the generalization performance of the proposed model at different test points, even when using a very small amount of training data. After doing several computational training with random weight initiation, the optimal model is achieved at an epoch number of 750. Finally, to evaluate the performance of the proposed model, we used different test data at different points. As shown in Fig. 4(b), the CNN-DE model with AE has better RMSE performance than without the AE model. Our proposed system achieves 4 times accuracy improvement overall. As a result, the well-trained model accurately detects the Bragg wavelength of each FBG. Therefore, the proposed hybrid of AE Pre-trained CNN and DE model significantly outperforms DE both in RMSE and in testing time. Moreover, the proposed hybrid of AE Pre-trained CNN and DE (AECNNDE) model can speed-up the computational time in a maximum of 30 times than the DE model.

4. Conclusion

In this paper, we proposed a novel interrogation system for the FBG sensor system. Thus, the spectra overlapping problem is solved by combining the DE algorithm and CNN techniques integrated with an unsupervised Autoencoder pre-training strategy. Moreover, the proposed sensor structure has a self-healing ability with an asymmetry coupler setup, and the high computational cost of the DE algorithm is reduced 30 times by introducing a CNN network. Finally, to improve the generalization ability of the proposed system even when a small amount of data is given, our network is pre-trained with an unsupervised autoencoder using un-labeled data. Therefore, the entire system can be initialized without human labeling, and the performance improves over time.

References

[1] Y. Mao, I. Ashry, T. K. Ng, and B. S. Ooi, "Towards early detection of red palm weevil using optical fiber distributed acoustic sensor, in *Proc. Opt. Fiber Commun. Conf.*, 2019.
[2] I. Ashry *et al.*, "A review of using few-mode fibers for optical sensing," *IEEE Access*, vol. 8, pp. 179592–179605, 2020.
[3] D. Barrera, V. Finazzi, J. Villatoro, S. Sales, and V. Pruneri, "Packaged optical sensors based on regenerated fiber Bragg gratings for high temperature applications," *IEEE Sensors J.*, vol. 12, no. 1, pp. 107–112, Jan. 2012.
[4] D. Chen, C. Shu, and S. He, "Multiple fiber Bragg grating interrogation based on a spectrum-limited Fourier domain mode-locking fiber laser," *Opt. Lett.*, vol. 33, 2008, Art. no. 1395.
[5] A. D. Kersey *et al.*, "Fiber grating sensors," *J. Light. Technol.*, vol. 15, no. 8, pp. 1442–1463, 1997.
[6] A. D. Kersey, T. A. Berkoff, and W. W. Morey, "Multiplexed fiber Bragg grating strain-sensor system with a fiber Fabry-Perot wavelength filter," *Opt. Lett.*, vol. 18, no. 16, 1993, Art. no. 1370.
[7] S. J. Mihailov, "Fiber Bragg grating sensors for harsh environments," *Sensors*, vol. 12, no. 2, pp. 1898–1918, 2012.
[8] C. Ghosh and V. Priye, "Augmentation of sensitivity of FBG strain sensor for biomedical operation," *Appl. Opt.*, vol. 57, no. 24, pp. 6906–6910, 2018.
[9] C. Ghosh and V. Priye, "Highly sensitive FBG strain sensor with enhanced measurement range based on higher order FWM," *IEEE Photon. J.*, vol. 12, no. 1, Feb. 2020, Art. no. 6800407.

[10] K. Yao *et al*., "Design and analysis of a combined strain–vibration–temperature sensor with two fiber bragg gratings and a trapezoidal beam," *Sensors*, vol. 19, no. 16, 2019, Art. no. 3571.
[11] Y. Hu, W. Mo, K. Dong, F. Jin, and J. Song, "Using maximum spectrum of continuous wavelet transform for demodulation of an overlapped spectrum in a fiber Bragg grating sensor network," *Appl. Opt*., vol. 55, no. 17, pp. 4670–4675, 2016.
[12] W. Zhang, M. Zhang, Y. Lan, Y. Zhao, and W. Dai, "Detection of crack locations in aluminum alloy structures using FBG sensors," *Sensors*, vol. 20, no. 2, p. 347, 2020.
[13] P. C. Peng and K. Y. Huang, "Fiber Bragg grating sensor system with two-level ring architecture," *IEEE Sensors J*., vol. 9, no. 4, pp. 309–313, Apr. 2009.
[14] K. S. Choi *et al*., "Improved spectral tag method for FBG sensor multiplexing with equally spaced spectral codes and simulated annealing algorithm," in *Proc. IEEE Sensors*, 2009, pp. 1256–1259.
[15] P. C. Peng, J. H. Lin, H. Y. Tseng, and S. Chi, "Intensity and wavelength-division multiplexing FBG sensor system using a tunable multiport fiber ring laser," *IEEE Photon. Technol. Lett*., vol. 16, no. 1, pp. 230–232, Jan. 2004.
[16] Y. C. Manie *et al*., "Enhancement of the multiplexing capacity and measurement accuracy of FBG sensor system using IWDM technique and deep learning algorithm," *J. Light. Technol*., vol. 38, no. 6, pp. 1589–1603, 2020.
[17] L. Zhang, Y. Liu, J. A. R. Williams, and I. Bennion, "Enhanced FBG strain sensing multiplexing capacity using combination of intensity and wavelength dual-coding technique," *IEEE Photon. Technol. Lett*., vol. 11, no. 12, pp. 1638–1640, Dec. 1999.
[18] Y. C. Manie *et al*., "Intensity and wavelength division multiplexing FBG sensor system using a Raman amplifier and extreme learning machine," *J. Sensors*, vol. 2018, 2018.
[19] Y. C. Manie *et al*., "Using a machine learning algorithm integrated with data de-noising techniques to optimize the multipoint sensor network," *Sensors*, vol. 20, 2020, Art. no. 1070.
[20] H. Jiang, J. Chen, T. Liu, and W. Huang, "A novel wavelength detection technique of overlapping spectra in the serial WDM FBG sensor network," *Sensors Actuators A: Phys*., vol. 198, pp. 31–34, 2013.
[21] B. Li *et al*., "Robust convolutional neural network model for wavelength detection in overlapping fiber bragg grating sensor network," in *Proc. Opt. Fiber Commun. Conf*., 2020.
[22] P. C. Peng, J. B. Wang, and K. Y. Huang. "Reliable fiber sensor system with star-ring-bus architecture," *Sensors*, vol. 10, no. 5, pp. 4194–4205, 2010.
[23] H. W. Gu *et al*., "Hexagonal mesh architecture for large-area multipoint fiber sensor system," *IEEE Photon. Technol. Lett*., vol. 26, no. 18, pp. 1878–1881, Sep. 2014.
[24] K. M. Feng, C. Y. Wu, J. H. Yan, C. Y. Lin, and P. C. Peng, "Fiber bragg grating-based three-dimensional multipoint ring-mesh sensing system withrobust self-healing function," *IEEE J. Sel. Topics Quantum Electron*., vol. 18, no. 5, pp. 1613–1620, Sep./Oct. 2012.